Two oligopeptide transporters from *Caenorhabditis elegans*: molecular cloning and functional expression

You-Jun FEI[1], Takuya FUJITA, David F. LAPP, Vadivel GANAPATHY and Frederick H. LEIBACH
Department of Biochemistry and Molecular Biology, Medical College of Georgia, Augusta, GA 30912, U.S.A.

Two novel oligopeptide transporter cDNA clones, CPTA and CPTB, were identified by screening a *Caenorhabditis elegans* cDNA library using homology hybridization. The transporter proteins deduced from the cDNAs possess multiple transmembrane domains and reveal a moderate similarity to their mammalian counterparts in amino acid sequences. CPTA and CPTB, when expressed in *Xenopus laevis* oocytes and studied by both radiotracer flux and microelectrode voltage-clamp protocol, displayed a saturable electrogenic transport activity driven by a proton gradient with an overlapping broad spectrum of substrate specificity. Both transporters recognize di-, tri- and tetra-peptides including phenylalanylmethionylarginylphenylalaninamide (FMRFamide) and *N*-acetylaspartylglutamate, members of a large neuropeptide family commonly found throughout the animal kingdom. Kinetic analysis, however, revealed that CPTA and CPTB differed in their affinity for the peptide substrates, the former being a high-affinity type and the latter a low-affinity type. CPTA and CPTB are encoded by two distinct genes localized on separate chromosomes and are expressed during the whole life span of the organism.

INTRODUCTION

Peptide transport across the cell membrane as one of many transmembrane activities is mediated by specific integral membrane proteins (carriers) and has been demonstrated to be a widely distributed phenomenon throughout Nature in both prokaryotes and eukaryotes, such as bacteria, yeasts, plants and animals [1]. Peptide transporters (PEPT) play two major roles in animals; absorption of small peptides in the epithelial cells of intestinal tract and kidney tubules and re-uptake of neuropeptide degradation products in the nervous system [2–4]. A comprehensive knowledge of the nutrition-related functions of the PEPTs was obtained in the past decade through biochemical and molecular biological studies [5–12]. These studies have led to the identification of two distinct peptide transporters, PEPT1 and PEPT2, which are expressed in the intestine and /or kidney. These transporters are unique in mammalian systems because of their dependence on a transmembrane H^+ gradient rather than a Na^+ gradient as the driving force. In addition to their natural substrates, the mammalian PEPT systems are also capable of transporting several pharmacologically active compounds including β-lactam antibiotics, the anti-tumour agent bestatin, angiotensin converting enzyme inhibitors and renin inhibitors [2,3]. The potential for nutritional, clinical and therapeutic applications of the PEPT systems necessitates a clear understanding of the biochemical and molecular aspects of the carrier proteins responsible for this process.

At present little is known about the second major putative role of the PEPT system as a neurotransmitter-related membrane transporter. Recently Yamashita et al. [4] isolated a third member, peptide/histidine transporter (PHT1), of the growing PEPT family from a rat brain cDNA library. The cloning and characterization of PHT1, the first neuro-specific PEPT member, is definitely a prelude for a more extensive investigation of the possible roles played by the PEPT system in the neuropeptide regulation and catabolic pathway.

Over the past two decades, the nematode *Caenorhabditis elegans* has become one of the leading model systems used to exploit a great variety of topics in biology and medicine due to its favourable experimental attributes and the wealth of information available in the literature on various aspects of this organism [13–15]. The presence of at least two putative peptide transporters, CPTA and CPTB, in *C. elegans* was implied by database searches with the BLAST algorithms against the *C. elegans* genomic DNA sequences [14]. An amino acid sequence comparison between either the predicted CPTA or CPTB and the mammalian PEPTs demonstrated a moderate similarity, which established the foundation of our cloning work of the PEPT systems in *C. elegans*. The two novel PEPT members from *C. elegans* were isolated by a homologous hybridization and characterized by a combination of radiotracer flux and electrophysiological studies in transporter-expressing *Xenopus* oocytes.

MATERIALS and METHODS

Nematode culture

A wild nematode strain, *C. elegans* N2 (Bristol), was obtained from the *Caenorhabditis* Genetics Center (St. Paul, MN, U.S.A.). Nematode culture was by a standard procedure with a large-scale liquid cultivation protocol. To remove the main contaminants, the nematodes were cleaned by sedimentation through

Abbreviations used: CPT, *C. elegans* peptide transporter; FMRFamide, phenylalanylmethionylarginylphenylalaninamide; PEPT, peptide transporter; PHT1, peptide/histidine transporter; NAAG, *N*-acetylaspartylglutamate; RT-PCR, reverse transcription-PCR; Gly-Sar (GS), glycylsarcosine; POT, proton-coupled oligopeptide transporter; TM, transmembrane domain.

[1] To whom correspondence should be addressed (email: yjfei@mail.mcg.edu).

The nucleotide sequence data reported have been deposited in the EMLB, GenBank and DDBJ nucleotide sequence databases under accession numbers AF000417 (CPTA) and AF00418 (CPTB).

15% (w/v) Ficoll 400 in 0.1 M NaCl. The pellet was then homogenized for total RNA preparation. To obtain homogeneous *C. elegans* subpopulations containing different developmental stages, synchronously growing animals were prepared using the alkaline hypochlorite method [16].

Extraction and purification of poly(A)$^+$ RNA

Total RNA was isolated from the *C. elegans* using an RNA isolation kit (RNAzol; Cinna/Biotecx Laboratories Inc., Houston, TX, U.S.A.). Poly(A)$^+$ mRNA was purified by double-affinity chromatography using oligo(dT)-cellulose (ClonTech, Palo Alto, CA, U.S.A.).

Reverse transcription (RT)-PCR

Two pairs of the PCR primers specific for the putative *C. elegans* peptide transporters were designed: 5′-TCA CAC CTT CAC GAT GAC-3′ (forward primer for CPTA) and 5′-GAT GAG TGG ATG AGG ATG-3′ (reverse primer for CPTA); 5′-TGA CAT TCT ACC TGC TTA AC-3′ (forward primer for CPTB) and 5′-CAA GAA CAT GAC AAG AAC AC-3′ (reverse primer for CPTB). Poly(A)$^+$ RNA (~ 0.5 μg), isolated from mixed stage *C. elegans* worms, was taken as a template to perform RT-PCR (RT-PCR kit; Perkin Elmer, Norwalk, CT, U.S.A.). A single DNA fragment was obtained by RT-PCR for both CPTA and CPTB with an estimated size of ~ 0.8 kbp as predicted by the primers. Following PCR, the amplified DNA fragments were purified by Centricon-30 (Amicon Inc., Beverly, MA, U.S.A.) and cloned into a TA-vector (Novagen, Madison, WI, U.S.A.). These two DNA fragments were used to screen the cDNA library.

Construction of a directional *C. elegans* cDNA library

The SuperScript Plasmid System (GIBCO BRL) was used to establish the cDNA library using the poly(A)$^+$ RNA from *C. elegans*. The transformation of the ligated cDNA into *Escherichia coli* was performed by electroporation using ElectroMAX DH10B-competent cells. Routine procedures were used for bacterial plating, filter lifting, DNA fragment labelling and the hybridization methods [17]. The DNA sequencing of the full-length CPTA and CPTB clones was performed using an automatic PCR thermocycler procedure.

In vitro transcription of cRNA, oocyte expression and electrophysiological studies

In vitro transcription, oocyte injection, uptake assay with a prototypical substrate for the peptide transporter, [2-^{14}C]glycyl[1-^{14}C]sarcosine (Gly-Sar, GS) and kinetic studies of the peptide transporters expressed in oocytes using a conventional two microelectrode voltage clamp method were as described previously [5,18].

Analysis of developmental stage expression of the CPTA and CPTB genes

A semi-quantitative RT-PCR assay using the same CPTA- and CPTB-specific primers described in the previous section, with minor modifications, was used to study the developmental stage expression and to estimate the abundance of the CPTA and CPTB messages at different stages. Total RNA from each stage was quantified by an internal control reaction initiated by a pair of primers specific for actin IV protein (the forward primer for actin: 5′-TGA CCC AAA TCA TGT TCG AGA-3′ and the reverse primer for actin: 5′-TGA CAC CAT TCT CAG AGT CGA-3′) and was run simultaneously, in parallel, under the same conditions as those used for the quantification of CPTA and CPTB transcripts. The quantity of the template total RNA and the thermocycle number in the PCR were predetermined by titration. The template total RNA used was 125 ng for each stage throughout the experiments and 30 cycles were used for the PCR. An excessive primer concentration (50 pmol) for both forward and reverse primers was employed to fully convert the template mRNA molecules into the first strand cDNA. In addition to 200 μM dNTPs, 2.0 μCi [α-^{32}P]dCTP (3000 Ci/mmol; Amersham, Arlington Heights, IL, U.S.A.) was included during the PCR. The resultant PCR products were resolved in an 1.0% (w/v) agarose gel, the gel was dried and autoradiograms were made following electrophoresis. The intensity of the radioactive fragments was measured using a scanning densitometer (Shimadzu, Columbia, MD, U.S.A.).

RESULTS AND DISCUSSION

Molecular cloning and the structural aspects of CPTA and CPTB

Two DNA fragments (~ 0.8 kbp long), cpta and cptb, were obtained by an RT-PCR method using two primer sets designed according to the cosmid insert sequences (lower case indicates that they are partial clones). The DNA sequences of cpta and cptb matched respectively to those of CPTA (from Ser-4 to Gln-261) and CPTB (from Thr-18 to Lys-305) at the protein level, as suggested by the GenFinder from the genome [14,15]. The PCR clones cpta and cptb were used as hybridization probes to screen a *C. elegans* (mixed stages) cDNA library to obtain full-length cDNA clones. The CPTA gene from *C. elegans* is localized on chromosome IV and contains at least ~ 4.0 kbp nucleotides. The CPTB gene is localized on chromosome X (*C. elegans* database, ACeDB, version 4.3, Data version WS2.4-16) and contains ~ 4.8 kbp nucleotides (excluding the unidentified promoter region). The presence of 17 exons in the CPTA gene and 14 exons in the CPTB gene is deduced by comparison of the sequences of the cloned cDNAs and the GenBank deposit (C06G8.2 and K03E7 respectively) reported by the nematode genome sequence project teams. The gene structures of CPTA and CPTB with the exons and the corresponding introns are shown in Figure 1. Although more than half of the *C. elegans*

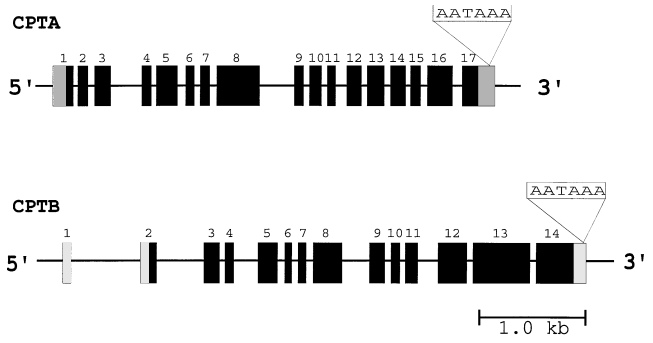

Figure 1 Structure of CPTA and CPTB genes

Exons are indicated by filled boxes and numbered accordingly; introns are indicated by horizontal lines. The untranslated regions in exons are indicated by stippled boxes. The consensus polyadenylation signal, AATAAA, is also shown. Sizes and positions of the exons and the introns in the figure are drawn to scale.

CPTA

```
  1  MGASHLHDDP RPGSPVDHQP TTWGGIIKKW PKQTFLIVGN ELCERFSFYG
 51  MRAVLTLYFF NILNFSQSFS TVLFHAETVI CYSSPLLGSI LADGYIGKFW
101  TIFFISIFYA CGQILLAFSS IAPSGSSHHP LLDLLGLLIV GLGTGGIKPC
151  VSAFGGDQFP AHYTRMISLF FSMFYFSINA GSLISMWLTP YFRSMSCFGH
201  DSCYPLAFGI PAILMIVATL VFMAGSFWYK KVPPKENIIF KVIGTITTAL
251  RKKASSSSTH QRSHWLEYSL DGHDCALSTE CKNLHGNCAQ RRYIEDIKRL
301  FRVLVMMIPV PMFWALVDQQ GSTWVLQAVG MDAKVFGFEI LPDQMGVLNA
351  FLILFFIPIF QSIVYPTIEK LGFQMTMLRK MAGGGILTAV SFFVCGIVQL
401  FVNPTLPYIP MANEAHLTII NTIPSCDFNV LIDSREPFDL LRKSGIAPDD
451  SVRKPISFTG DDFFQPNITF DNLAPNCPKF TAKPMLAPAT SYVLTLSPNG
501  WAYNAVRPEK PKSGKGELSM GLNLIVPCDK IPSNVTWEQC NGTEGYSGAI
551  ALCKVESDVI TDNNNVCDPT AKGKFYVLSN ANPLDVHDFS KKSTVTAFGR
601  TYSPIEMKPG TYRLFYTDDS RTHFTPLNLP PVQQDHMGGQ YLITVSTRSK
651  NDSEVLATTE SLVSYNRVSI LWQIPQYVIL TAGEVLFSIT GLEFAYTEAS
701  PQLKSVVQAL WLFTTAIGDL IVVVIEMLNI FSDVAVQMFV FGGIMLFVIF
751  VFILLAVFYY EYADYSNESE VLTEKMIVDD DHTRI*
```

CPTB

```
  1  MIRHWPKTTL CIVSNEFCER FSYYGMRTVL TFYLLNVLKF TDSQSTIFFN
 51  GFTVLCYTTP LLGSIVADGY IGKFWTIFSV SILYAIGQVV LALASTKNFQ
101  SSVHPWMDLS GLLIIAFGTG GIKPCVSAFG GDQFELGQER MLSLFFSMFV
151  FSINAGSMIS TFISPIFRSQ PCLGQDSCYP MAFGIPAILM IVATLVFMGG
201  SFWYKKNPPK DNVFGEVSRL MFRAVGNKMK SGSTPKEHWL LHYLTTHDCA
251  LDAKCLELQA EKRNKNLCQK KKFIDDVRSL LRVLVMFLPV PMFWALVDQQ
301  GSVWLIQAIQ MDCRLSDTLL LLPDQMQTLN AVLILLLFIPL FQVIIYPVAA
351  KCVRLTPLRK MVTGGLLASL AELLTGFVQL QVNTTLPTLP EEGEASISFW
401  NQFETDCTIT VMSGIHKRVL PHDKYLHEDK KNKSGIYNLF TTKSPAKGNG
451  DWTLTYDLSY DGACGDTSKL EKTVKVTAKS KKIIYVGVGS FGYYQNTANT
501  DKPTDGTGEF SMGIVTVFNS SYGGNFAMCR QNTSDFDVNH PCNPRHPADF
551  YFWETDYNSH TDDRDQNATI TGSLSSQPAV TYKQKSVKPG YWQLYYLLNT
601  PKDVDRQTYN KTATLVAPTN YGFHRVKQGG VFIYALTGTY ENPKIHELQI
651  VQSNSVSLLW QIPQIVVITA AEILFSITGY EFAYSQSAPS MKALVQALWL
701  LTTAAGDSLI VVITILNLFE NMAVEFFVYA AAMFVVIAIF ALLSIFYYTY
751  NYYTTDEEDG EIGVDDEEEI EDHNPRYSID NKGFHPDEKD TFDMHF*
```

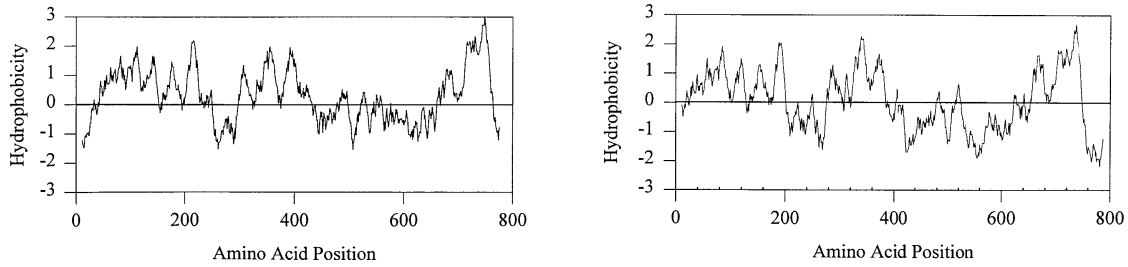

Figure 2 Amino acid sequences of CPTA and CPTB

The amino acid positions are marked on the left side of each protein sequence. TMs determined by hydrophobicity plot (shown below each sequence panel) are underlined. Stop codons are indicated by an asterisk (*).

gene products were trans-spliced [19], it was not possible to identify the transplicing leader DNA sequences, SL1 and SL2, in the cDNAs, which indicates that the mRNA species encoding the CPTA and CPTB are directly transcribed from the corresponding genes.

The cDNA sequences of both CPTA and CPTB were approx. 2.6 kbp long with poly(A) tails. The 5′-untranslated regions were 121 and 147 bp long in CPTA and CPTB respectively. The 3′-untranslated regions were 176 and 141 bp long in CPTA and CPTB respectively. A polyadenylation signal sequence AATAAA was found in both cDNA clones.

The CPTA transporter protein deduced from the cDNA sequence contained 785 amino acid residues and had a molecular mass of ~ 87.6 kDa, with an isoelectric point of 6.64. According to the Kyte–Doolittle hydropathy plot, this protein possessed 11 transmembrane domains (TMs), with a window size of 21 amino acids (Figure 2). The huge extracellular loop was predicted to be located between TM8 and TM9.

The CPTB transporter protein deduced from the cDNA sequence contained 796 amino acid residues and had a molecular mass of ~ 89.7 kDa, with an isoelectric point of 6.41. CPTB transporter protein also possessed 11 TMs. The huge extracellular loop was located between TM 8 and TM 9. A leucine zipper-like structure was found on TM7, which consists of a periodic repetition of leucine residues at every sixth to seventh position over the whole transmembrane fragment. The relationship between the unique leucine zipper-like structure, which is usually found in some members of the nuclear DNA-binding protein family, and the peptide transport activity of CPTB remains to be explored.

A multiple sequence analysis of the PEPT family members indicates that sequence identity/similarity is more frequently presented in the TMs than in the intra- or extra-cellular loops. Three highly conserved homologous amino acid stretches identified among the proton-coupled oligopeptide transporter (POT) family members, namely consensus sequences I, II and III, are partly conserved in CPTA and CPTB. Consensus sequence I, GX{2}IADXWLGXFXTIX{5}VX{3}G, corresponds to the region from Gly-88 to Gly-112 in CPTA. Consensus sequence II, GTGGIKPXV, encompasses a stretch from Gly-143 to Val-151 in CPTA. Consensus sequence III, FX{2}FYLXINXGSL, is located from Phe-171 to Leu-183 [1]. These observed unique regions are situated in the first five TMs, which implies that the first several TMs are highly preserved during the evolution and associated with some hitherto unidentified important functions that are common to all PEPTs.

A mandatory histidine residue, corresponding to His-75 in CPTA, is conserved in all mammalian PEPT subfamily members and its obligatory role in the proton-coupled peptide transporter function has been verified by site-directed mutagenesis [20]. This crucial histidine residue is absent in CPTB and is replaced by an asparagine residue. In the present studies, the CPTB showed an unusually high peptide transport activity with an electrogenic property, despite the lack of the highly conserved histidine residue. The molecular basis of the absence of this histidine residue in CPTB remains to be determined.

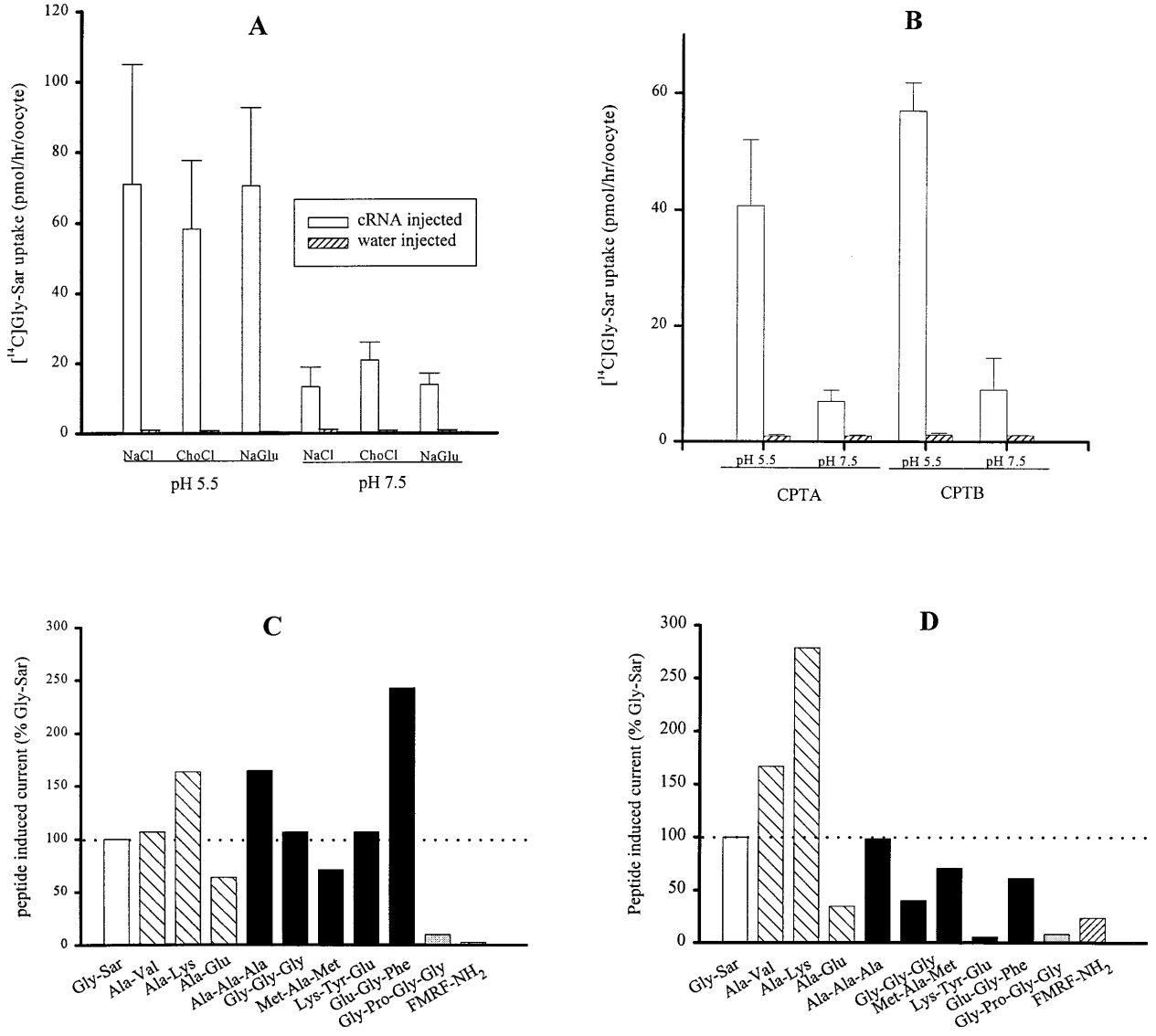

Figure 3 pH-Dependence and substrate specificity of CPTA and CPTB

[^{14}C]Gly-Sar (30 μM) flux assay (1 h) was performed with individual cRNA-injected oocytes 4–6 days after injection. Values represent the mean $\pm$ S.E.M (n = 8–10 oocytes). (**A**) Na^+- and Cl^--independent nature of transport activity of CPTA at pH 5.5 and pH 7.5. Bars labelled ChoCl and NaGlu indicate the uptake activity in Na^+-free buffer and in Cl^--free buffer respectively. The values (hatched bars) obtained from the water-injected oocytes are also shown. (**B**) shows that the transport activity is proton dependent for both CPTA and CPTB. The substrate specificity was determined by measuring the current induced by each substrate (labelled below the bars), applied in the perfusing chamber, using a voltage-clamp protocol. The substrate-induced current was expressed as a percentage of that of Gly-Sar. The concentration for all substrates was 1 mM, except for FMRFamide (0.5 mM). (**C** and **D**) show the substrate-specificity profiles for CPTA and CPTB respectively. The values are the means of three experiments; error bars are omitted for clarity.

The presence of PEPT in such an extensive array of animal phyla, from nematodes to humans, suggests that the different PEPTs evolved from a common ancestral gene, performed a common function throughout the animal kingdom, possessed certain indispensable elements in their basic molecular structure and retained the resemblance among individual members during the evolution. The fact that *C. elegans* possesses two subtypes of PEPTs, one with high affinity and the other with low affinity, implies that divergence between a high-affinity PEPT and a low-affinity PEPT is an ancient event in evolution. Recently, a database search revealed that there might be another isoform of the peptide transporter encoded by gene F56F4.5 on chromosome I in *C. elegans*.

The driving force and substrate specificity

Transport activity of CPTA and CPTB is H^+-dependent and Na^+- and Cl^--independent (Figures 3A and 3B). At pH_{out} 5.5, Gly-Sar uptake by the CPTA cRNA-injected oocytes showed a 43-fold increase compared with that of water-injected oocytes. The CPTB cRNA-injected oocytes showed an even higher uptake value, a 50-fold increase. In an alkaline environment (pH_{out} 7.5),

Table 1 Amino acid sequence comparison of the high- and low-affinity peptide transporters from human and *C. elegans*

The comparison between human (h) and *C. elegans* amino acid sequences was made using the BESTFIT program (GCG package, Madison, WI, U.S.A.). The percentage similarity and identity (in parentheses) are shown.

	hPEPT2	CPTA	CPTB
hPEPT1	69.4 (49.5)	61.7 (40.1)	62.8 (36.9)
hPEPT2	–	60.3 (36.0)	62.1 (37.5)
CPTA	–	–	67.3 (46.6)

the uptake activity in both CPTA and CPTB cRNA-injected oocytes decreased dramatically. Uptake activity from the same batch of oocytes injected with CPTA cRNA at pH_{out} 5.5 compared with that at pH_{out} 7.5 was significantly different (Figure 3B). Similar results were obtained in the CPTB cRNA-injected oocytes (Figure 3B).

Substitution of Na^+ by choline and substitution of Cl^- by gluconate did not cause a significant change in the activity of CPTA at either pH_{out} 5.5 or pH_{out} 7.5 (Figure 3A). The uptake (means $\pm$ S.E.M.) of [^{14}C]Gly-Sar by the CPTA cRNA-injected oocytes in an uptake buffer containing 100 mM NaCl (pH 5.5) (71.0 ± 33.9 pmol/h per oocyte) was similar to the values obtained in the absence of Na^+ or Cl^- (58.2 ± 19.3 and 70.4 ± 22.2 pmol/h per oocyte). Similar profiles of the uptake activity for [^{14}C]Gly-Sar at pH 7.5 were obtained using another batch of oocytes. In the presence of both Na^+ and Cl^-, the CPTA-expressing oocytes showed transport activity, 13.3 ± 5.6 pmol/h per oocyte, which was not significantly different from those in the absence of Na^+ or Cl^- (20.9 ± 5.1 pmol/h per oocyte and 13.9 ± 3.2 pmol/h per oocyte respectively). The Na^+- and Cl^--independent nature was also demonstrated in the oocytes expressing CPTB (results not shown). From these data, it was concluded that transport activity of both CPTA and CPTB was driven by an inwardly directed H^+ gradient and was independent onf Na^+ and Cl^-.

These two isoforms of PEPT displayed a broad spectrum of substrate specificity. They recognized di- and tri-peptides and, to a minor extent, tetrapeptides (Figures 3C and 3D). The substrate specificity was determined by the two microelectrode voltage clamp procedure, using 1.0 mM substrates with the transporter-expressing oocytes, and the substrate-induced current was measured. The CPTA (Figure 3C) and the CPTB (Figure 3D) transport activity is shown. Several peptides containing two, three or four amino acids were found to be substrates for both CPTA and CPTB. A number of amino acids were also tested including histidine, lysine, leucine, glutamate, glutamine, phenylalanine and alanine; none of them was found to be a substrate for the *C. elegans* PEPTs. This is in obvious contrast to the substrate specificity of a recently cloned proton-coupled oligopeptide transporter, PHT1, from rat brain [4], which recognized oligopeptides as well as the amino acid histidine as substrates. PHT1 revealed a low similarity at the level of amino acid sequence to members of the mammalian PEPT family. It showed $\sim 17\%$ identity and $\sim 32\%$ similarity with the low-affinity PEPT1s and $\sim 12\%$ identity and $\sim 27\%$ similarity with the high-affinity PEPT2s [4]. CPTA and CPTB from *C. elegans* demonstrated a closer relationship with PHT1 than any of the mammalian POT members, $\sim 26\%$ identity and $\sim 55\%$ similarity, and $\sim 25\%$ identity and $\sim 52\%$ similarity respectively. From an evolutionary point of view, CPTA and CPTB are more intimately related to the mammalian PEPT subgroup in the POT superfamily (with a higher percentage of identity and similarity, ~ 36–47% and ~ 60–69% respectively) and reside in a middle branch between the PEPT subgroup and another subgroup, where PHT1 belongs within the POT superfamily (Table 1).

At present, little is known about the requirement for a free C-terminus in the peptide substrates of PEPTs. To our surprise, a C-terminal blocked tetrapeptide phenylalanylmethionylarginyl-phenylalaninamide (FMRFamide) was an excellent substrate for CPTB. Figure 3(D) shows that FMRFamide, amidated at the C-terminus, was recognized by CPTB with current magnitude about $\sim 24\%$ of Gly-Sar. In comparison with CPTB, CPTA exhibited little, if any, uptake activity towards FMRFamide (Figure 3C). Since numerous FMRFamide-related peptides isolated from nematodes have a common C-terminal arginyl-phenylalaninamide motif for biological activities [21], a transporter recognizing this tetrapeptide is, therefore, of special significance.

Michaelis–Menten kinetic model and co-operative mechanism

The transport process mediated by CPTA from *C. elegans* exhibited electrogenicity and dependence on membrane potential and substrate concentration. The substrate-induced current was saturable and followed Michaelis–Menten kinetics. In Figure 4(A), the membrane currents induced at different concentrations of Gly-Sar and at three different membrane potentials (-50, -70 and -110 mV) are shown. At a given substrate concentration, the evoked current depended upon the testing voltage: the more negative the membrane potential, the higher the evoked membrane current. The dependence of the maximal substrate-induced current on the testing membrane potential (V_{test}) is displayed in Figure 4(B). The I_{max}^{GS} decreased as the testing membrane potential changed from -110 mV to -30 mV. The data also show the apparent high affinity (approx. 0.3 mM at -50 mV) and low capacity ($I_{max}^{GS} \sim 30$ nA) for CPTA compared with the low affinity peptide transporter CPTB, which showed very high capacity ($I_{max}^{GS} \sim 2000$ nA). The apparent affinity for substrate, $K_{0.5}^{GS}$, of the transporter CPTA exhibited voltage-dependent characteristics; the value tended to increase with a more hyperpolarized membrane potential (Figure 4C).

The substrate-induced current in the oocytes expressing the peptide transporter CPTB also demonstrated a similar membrane-potential dependence. Figure 4(D) shows the substrate concentration versus current relationship at three membrane potentials (-70 mV, -90 mV and -130 mV). The maximal substrate-induced membrane current, I_{max}^{GS}, was plotted against the testing membrane potential in Figure 4(E). The same trend as that shown by CPTA was observed; it increased with a more hyperpolarized membrane potential. The apparent affinity for the substrate, $K_{0.5}^{GS}$, on the other hand, showed a different pattern from that exhibited by CPTA (Figure 4F); the value decreased with a more hyperpolarized membrane potential. The apparent affinity for the substrate Gly-Sar decreased dramatically when the membrane potential depolarized from -50 mV to $+10$ mV. Since the peptide transporter CPTB is driven by both an inwardly directed proton gradient ($\Delta\mu_H$) and an inside-negative membrane potential ($\Delta\Psi$), it is conceivable that, at an extreme hyperpolarized membrane potential (e.g. at -150 mV), the transporter activity reaches such a condition that a much lower substrate concentration will saturate its binding sites.

With regard to the requirement of a free α-amino group for an oligopeptide to be accepted as a substrate of PEPT transporter subgroup, we tested an N-terminal-blocked dipeptide, *N*-acetyl-aspartylglutamate (NAAG), an endogenous mammalian brain

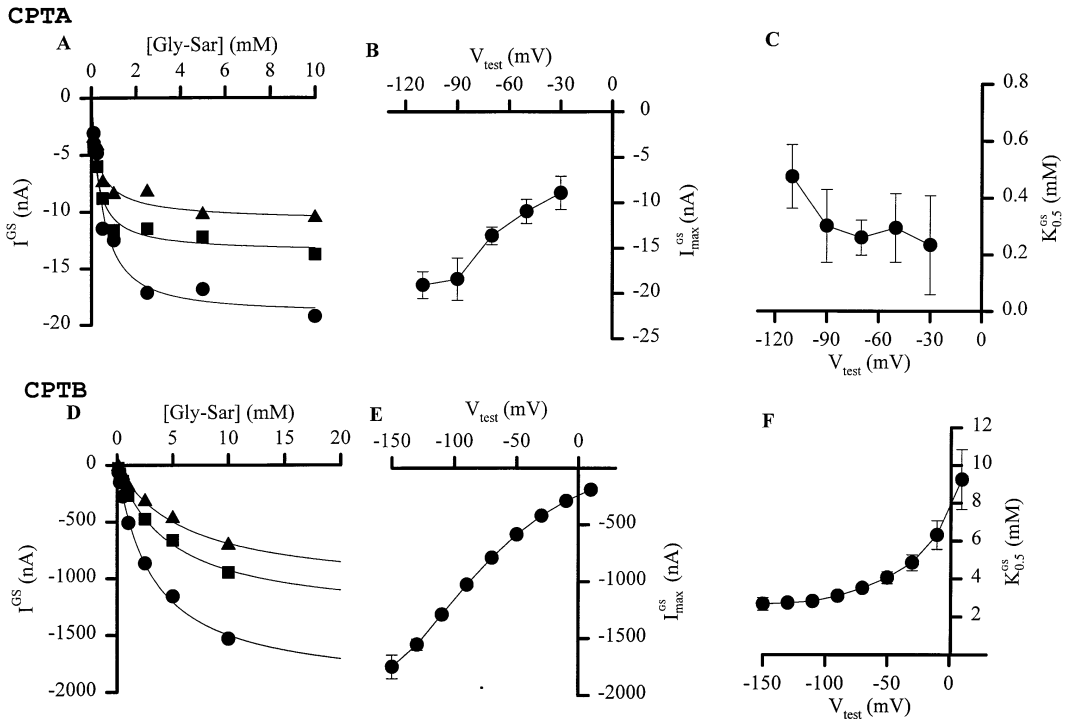

Figure 4 Substrate activation and its apparent affinity for CPTA and CPTB

(**A**) Substrate activation of CPTA at V_{test} −50 (▲), −70 (■) and −110 (●) mV respectively. A hyperbolic kinetic profile was evident at three different testing membrane potentials. (**B**) I^{GS}_{max} obtained using a saturating [GS], 10 mM, at pH 5.5. The I^{GS}_{max} is displayed as a function of V_{test}. (**C**) Apparent affinity of CPTA for Gly-Sar, $K^{GS}_{0.5}$, as a function of V_{test} (pH 5.5). (**D**, **E** and **F**) Parallel kinetic data set obtained from CPTB. The settings were the same as those for CPTA, except in (**D**) where the three V_{test} settings were −70 (▲), −90 (■) and −130 (●) mV respectively and the data were extrapolated to show the hyperbolic kinetic trend. The concentration of GS used in (**E**) was 10 mM.

peptide exhibiting a high affinity and specificity for a subsite of the brain *N*-methyl-D-aspartate receptor [22]. Our results demonstrated that NAAG is a preferred substrate for CPTA. Figure 5(A) shows a typical recording generated by different concentrations of NAAG in a CPTA-expressing oocyte. CPTA robustly transported NAAG with kinetic parameters (means ± S.E.M.) of $I^{NAAG}_{max} \sim 112.7 \pm 5.3$ nA and $K^{NAAG}_{0.5} \sim 1.0 \pm 0.1$ mM at a testing membrane potential of −50 mV. Transport efficiency for NAAG was shown to be ~10-fold higher than that of the prototype substrate for the PEPT subfamily, Gly-Sar. Using the same experimental conditions, Gly-Sar gave rise to a I^{GS}_{max} of $\sim 11.0 \pm 1.3$ nA.

Previous studies have shown that NAAG is found in high concentrations (0.5 μmol/g) in mammalian brain [23]. Little information is available regarding the presence and the potential physiological functions of NAAG in nematodes. Undoubtedly, our electrophysiological data of the NAAG kinetics conducted in CPTA-expressing oocytes will stimulate further studies in this area.

Because of the robust activity of CPTB, detailed studies on its transport kinetics were carried out. Figure 5(B) shows the I/V curves obtained at several different pH_{out} values using 5.0 mM Gly-Sar. The substrate-induced current, at a fixed substrate concentration, is a function of the testing voltage and proton concentration. Once again, the substrate-induced current was shown to be voltage- and proton-dependent: the more negative the membrane potential and the higher the proton gradient (the lower pH_{out}), the higher the substrate-induced current. The I/V curves obtained at all pH_{out} values converged and approached zero at a depolarized membrane potential of +50 mV. Figure 5(C) shows the I/V curves obtained at a fixed proton concentration (pH 5.5) and various substrate concentrations. The substrate-induced current was a function of both testing membrane potential and the substrate concentration: the more negative the membrane potential and the higher the substrate concentration, the higher the substrate-induced current. The I/V values obtained for each Gly-Sar concentration again converged and approached zero at a depolarized membrane potential of +50 mV.

The nature of the proton activation of CPTB could be observed by varying the pH_{out} value when Gly-Sar was applied at a subsaturating concentration, 10.0 mM. At each of the testing voltages shown in Figure 5(D), a hyperbolic curve, analogous to the substrate activation curves (Figures 4A and 4D), was observed with a Hill coefficient of ~1, suggesting that one H^+ binds to CPTB per transport cycle.

The value of $K^{H}_{0.5}$ at a testing membrane potential of −30 mV was 1.13 ± 0.20 μM (mean ± S.E.M.). The value decreased with an increasingly more negative test membrane potential (hyperpolarization) for all of the testing substrate concentrations and increased with an increasing depolarized membrane potential (towards a more positive membrane potential) (Figure 5E). At more hyperpolarized membrane potentials, the differences of $K^{H}_{0.5}$ between different substrate concentrations seem to be less obvious than at more depolarized membrane potentials.

Figure 5(F) shows the pH-dependence and membrane-potential dependence of the apparent affinity for Gly-Sar; the $K^{GS}_{0.5}$ value increased with a more positive membrane potential and with a higher pH_{out}. At −30 mV, $K^{GS}_{0.5}$ was 4.3 ± 0.9 (pH 5.0), 10.2 ± 0.7 (pH 6.0) and 15.2 ± 2.8 (pH 6.5) mM; at −110 mV,

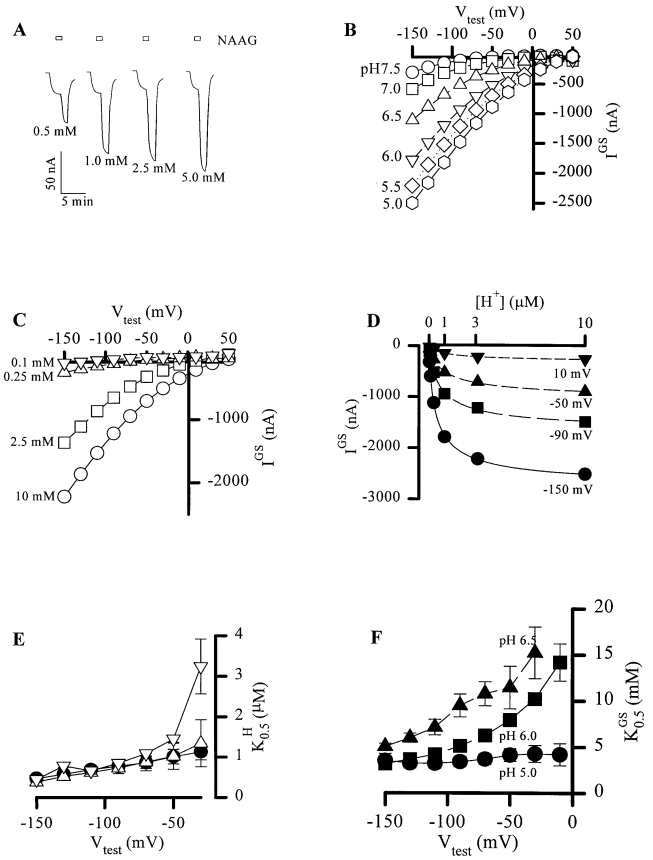

Figure 5 Kinetic features of CPTA and CPTB

(**A**) Representative recording of the NAAG-induced inward current at different concentrations (at pH 5.5) in a single CPTA-expressing oocyte. (**B**) *I*/*V* relationship of CPTB generated by varying the pH_{out} (shown on graph) at a fixed [GS] of 10 mM. (**C**) *I*/*V* relationship of CPTB generated by varying [GS] (shown on graph) at a fixed pH_{out}, pH 5.5. (**D**) Proton activation data of CPTB. Four representative curves at V_{test} −150, −90, −50 and 10 mV show the dependence of the 5.0 mM Gly-Sar-evoked current (I^{GS}) on the external proton concentration $[H^+]$, determined at pH 8.0, 7.5, 7.0, 6.5, 6.0, 5.5 and 5.0. (**E**) Apparent affinity of CPTB for protons as a function of the V_{test} and [GS]. Data were obtained at three different [GS], 1 mM (▽), 5 mM (△) and 10 mM (●). (**F**) Apparent affinity of CPTB for Gly-Sar as a function of the V_{test} and $[H^+]$. Data were obtained at three different pH_{out}, pH 6.5 (▲), pH 6.0 (■) and pH 5.0 (●).

$K^{GS}_{0.5}$ decreased to 3.1 ± 0.6 (pH 5.0), 4.2 ± 0.1 (pH 6.0) and 7.1 ± 0.9 (pH 6.5) mM respectively.

Kinetic studies of CPTB indicated a positive co-operativity relationship between H^+ and the substrate Gly-Sar. Increasing $[H]^+_{out}$ and $[GS]_{out}$ increased the apparent affinity for Gly-Sar and H^+ respectively (Figures 5E and 5F), which suggests a simultaneous transport model. This positive co-operative mechanism was first reported in another proton-coupled sucrose co-transporter isolated from potato and analysed electrophysiologically [24]. This is in contrast to the 'sequential model' reported by Mackenzie et al. [18] and to the 'two-faced occlusion model' by Nussberger et al. [25] for the mammalian PEPT1.

Developmental stage-specific expression of CPTA and CPTB

To investigate the CPTA and CPTB expression levels during the different stages of *C. elegans* development, synchronized cultures were obtained and total RNA was isolated from each stage. The two isoforms of the peptide transporter were expressed during the whole life span as shown by the semi-quantitative RT-PCR

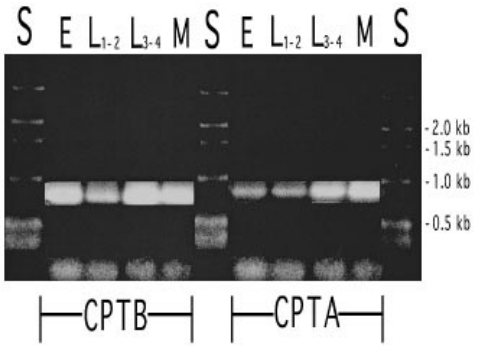

Figure 6 Developmental stage-specific expression of CPTA and CPTB

Following the RT-PCR reaction, 10 μl of the products were separated in a 1.0% (w/v) agarose gel to show the size and the intensity of α-[^{32}P]dCTP-labelled CPTA- and CPTB-specific fragments. An α-[^{32}P]dCTP-labelled 1.0 kb marker (S) (GIBCO-BRL) was used as a molecular mass standard. The PCR products (approx. 0.8 kbp for both CPTA and CPTB) from eggs (E), larval stages 1 and 2 (L_{1-2}), and 3 and 4 (L_{3-4}) and a mixed stage sample (M), with adult hermaphrodites being the predominant form in the population, are shown. The PCR products specific for actin IV (approx. 250 bp) (added manually) are shown under the CPT-specific fragments.

assay (Figure 6) on total RNA samples isolated from homogeneous *C. elegans* subpopulations at different developmental stages. A gradual increase in the expression level of CPTA during the development from embryo through larva L_{1-2} and L_{3-4} to adults was clearly evident. RT-PCR analysis of actin IV transcripts served as an internal control in these experiments. The relative intensities of the CPTA-specific product with respect to actin IV were 2.7, 2.7, 7.0 and 7.8 for the eggs, L_{1-2}, L_{3-4} and mixed stage animals respectively. In the case of CPTB, a biphasic expression pattern was seen. The expression seemed to reach a high level at the early stage (embryos), declined a little at stage of larva 1 and 2 and increased again when the animal was fully developed into the adult hermaphrodite. The relative intensities were 30.3, 4.5, 20.8 and 15.6 for the eggs, L_{1-2}, L_{3-4} and mixed stage animals respectively. The physiological significance of the two-peak pattern remains to be elucidated. Throughout the animal life span, the overall expression level of CPTB was consistently higher than that of CPTA. At the embryo stage, the CPTB/CPTA ratio was estimated to be ~ 11, and this value decreased to ~ 2 at the mixed stage. The considerably higher expression level of CPTB, especially during the embryonic development, in conjunction with its robust uptake activity leads us to postulate that the physiological functions of CPTB might be related to the nutritional roles.

This research is supported by National Institutes of Health grant DK28389 (F.H.L.), by a grant from the Medical College of Georgia Research Institute Inc., Augusta, GA 30912, U.S.A., and by a grant from the Biomedical Research Support Grant Program (B.R.S.G.), School of Medicine, Medical College of Georgia, Augusta, GA 30912, U.S.A. (Y.J.F.).

REFERENCES

1 Fei, Y. J., Ganapathy, V. and Leibach, F. H. (1998) Nucleic Acids Res. Mol. Biol. **58**, 239–261
2 Ganapathy, V., Brandsch, M. and Leibach, F. H. (1994) in Physiology of the Gastrointestinal Tract (Johnson, L. R., ed.), pp. 1773–1794, Raven, New York
3 Ganapathy, V. and Leibach, F. H. (1996) Curr. Opin. Nephrol. Hyperten. **5**, 395–400
4 Yamashita, T., Shimada, S., Guo, W., Sato, K., Kohmura, E., Hayakawa, T., Takagi, T. and Tohyama, M. (1997) J. Biol. Chem. **272**, 10205–10211

5 Fei, Y. J., Kanai, Y., Nussberger, S., Ganapathy, V., Leibach, F. H., Romero, M. F., Singh, S. K., Boron, W. F. and Hediger, M. A. (1994) Nature (London) **368**, 563–566
6 Boll, M., Markovich, D., Weber, W. M., Korte, H., Daniel, H. and Murer, H. (1994) Pflugers Archiv. Eur. J. Physiol. **429**, 146–149
7 Liang, R., Fei, Y. J., Prasad, P. D., Ramamoorthy, S., Han, H., Yang-Feng, T. L., Hediger, M. A., Ganapathy, V. and Leibach, F. H. (1995) J. Biol. Chem. **270**, 6456–6463
8 Liu, W., Liang, R., Ramamoorthy, S., Fei, Y. J., Ganapathy, M. E., Hediger, M. A., Ganapathy, V. and Leibach, F. H. (1995) Biochim. Biophys. Acta **1235**, 461–466
9 Saito, H., Okuda, M., Terada, T., Dadaki, S. and Inui, K. (1995) J. Pharmacol. Exp. Ther. **275**, 1631–1637
10 Boll, M., Herget, M., Wagener, M., Weber, W. M., Markovich, D., Biber, J., Clauss, W., Murer, H. and Daniel, H. (1996) Proc. Natl. Acad. Sci. U.S.A. **93**, 284–289
11 Miyamoto, K., Shiraga, T., Morita, K., Yamamoto, H., Haga, H., Taketani, Y., Tamai, I., Sai, Y., Tsuji, A. and Takeda, E. (1996) Biochim. Biophys. Acta **1305**, 34–38
12 Saito, H., Terada, T., Okuda, M., Sasaki, S. and Inui, K. (1996) Biochim. Biophys. Acta **1280**, 173–177
13 Chalfie, M. and White, J. (1988) in The Nematode *Caenorhabditis elegans* (Wood, W. B. and the Community of *C. elegans* Researchers, eds.), pp. 337–391, Cold Spring Harbor Laboratory, New York
14 Hodgkin, J., Plasterk, R. H. and Waterston, R. H. (1995) Science **270**, 410–414
15 Chalfie, M., Eddy, S., Hengartner, M. O., Hodgkin, J., Kohara, Y., Plasterk, R. H., Waterston, R. H. and White, J. G. (1995) Science **270**, 415–430
16 Lewis, J.A and Fleming, J. T. (1995) Methods Cell Biol. **48**, 4–27
17 Sambrook, J., Fritsch, E. F. and Maniatis, T. (1989) Molecular Cloning: A Laboratory Manual, pp. 8.3–8.82, Cold Spring Harbor Laboratory, New York
18 Mackenzie, B., Loo, D. D. F., Fei, Y. J., Liu, W., Ganapathy, V., Leibach, F. H. and Wright, E. M. (1996) J. Biol. Chem. **271**, 5430–5437
19 Pettitt, J. and Kingston, I. B. (1994) Dev. Biol. **161**, 22–29
20 Fei, Y. J., Wei, L., Prasad, P., Kekuda, R., Oblak, T. G., Ganapathy, V. and Leibach, F. H. (1997) Biochemistry **36**, 452–460
21 Maule, A. G., Bowman, J. W., Thompson, D. P., Marks, N. J., Friedman, A. R. and Geary, T. G. (1996) Parasitology **113**, S119–S135
22 Trombley, P. Q. and Westbrook, G. L. (1990) J. Neurophysiol. **64**, 598–606
23 Zaczek, R., Koller, K., Cotter, R., Heller, D. and Coyle, J. T. (1983) Proc. Natl. Acad. Sci. U.S.A. **80**, 1116–1119
24 Boorer, K. J., Loo, D. D. F., Frommer, W. B. and Wright, E. M. (1996) J. Biol. Chem. **271**, 25139–25144
25 Nussberger, S., Steel, A., Trotti, D., Romero, M. F., Boron, W. F. and Hediger, M. A. (1997) J. Biol. Chem. **272**, 7777–7785

Received 25 November 1997/16 February 1998; accepted 27 February 1998